Article

Orbital Views of the Electron Transport in Molecular Devices

Kazunari Yoshizawa, Tomofumi Tada, and Aleksandar Staykov

J. Am. Chem. Soc., **2008**, 130 (29), 9406-9413 • DOI: 10.1021/ja800638t • Publication Date (Web): 25 June 2008

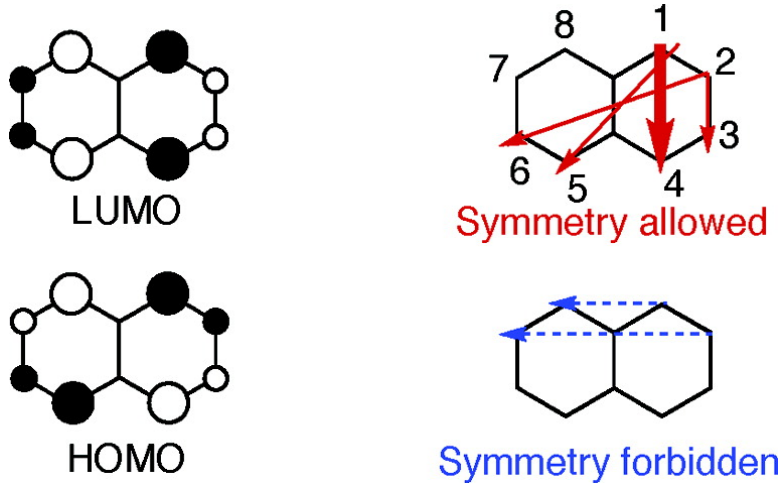

More About This Article

Additional resources and features associated with this article are available within the HTML version:

- Supporting Information
- Links to the 1 articles that cite this article, as of the time of this article download
- Access to high resolution figures
- Links to articles and content related to this article
- Copyright permission to reproduce figures and/or text from this article

View the Full Text HTML

J|A|C|S
ARTICLES

Published on Web 06/25/2008

Orbital Views of the Electron Transport in Molecular Devices

Kazunari Yoshizawa,*,† Tomofumi Tada,‡ and Aleksandar Staykov†

Institute for Materials Chemistry and Engineering, Kyushu University, Nishi-ku, Fukuoka 819-0395, Japan, and Department of Materials Engineering, The University of Tokyo, Bunkyo-ku, Tokyo 113-8656, Japan

Received January 25, 2008; E-mail: kazunari@ms.ifoc.kyushu-u.ac.jp

Abstract: Extended π-conjugated molecules are interesting materials that have been studied theoretically and experimentally with applications to conducting nanowire, memory, and diode in mind. Chemical understanding of electron transport properties in molecular junctions, in which two electrodes have weak contact with a π-conjugated molecule, is presented in terms of the orbital concept. The phase and amplitude of the HOMO and LUMO of π-conjugated molecules determine essential properties of the electron transport in them. The derived rule allows us to predict single molecules' essential transport properties, which significantly depend on the type of connection between a molecule and electrodes. Qualitative predictions based on frontier orbital analysis about the site-dependent electron transport in naphthalene, phenanthrene, and anthracene are compared with density functional theory calculations for the molecular junctions of their dithiolate derivatives, in which two gold electrodes have strong contact with a molecule through two Au−S bonds.

Introduction

Single-molecular devices that use unique electronic properties of a molecule or an ordered network of molecules have attracted much attention in nanoscale science and technology. Extensive studies on π-conjugated systems have been carried out theoretically and experimentally with applications to molecular wire, memory, and diode in mind. Landauer's formula[1] with Green's function techniques[2] is of great use for theoretical evaluation of electron transport phenomena in metal−molecule−metal junctions. Several important mechanisms that determine fundamental aspects of molecular conductance have been discussed as a function of molecular length, molecular conformation, and applied bias voltage.[3–11] In particular, conduction channel analysis in terms of orbital amplitude of the molecular orbitals near the Fermi energy have shown good guidelines in better understanding of molecular conductance. Orbital amplitude analysis based on first principles calculations reveals that the delocalization of orbital is important to make a good conduction pathway.[12–15]

We reported a close relationship between the frontier orbitals (highest occupied molecular orbital (HOMO) and lowest unoccupied molecular orbital (LUMO)) and the electron transport properties of π-conjugated systems.[16–18] The derived relationship describes the importance of orbital phase as well as amplitude of the HOMO and LUMO to determine essential features of the conductance in molecular junctions. Our orbital analysis uses zeroth Green's function for the molecular part of metal−molecule−metal junctions, in which two gold chains are assumed to have weak contact with a molecule. On the basis of chemical analysis of the phase and amplitude of the HOMO and LUMO, we are able to predict possible connections for effective electron transport in π-conjugated systems. The connection dependence on the transport properties in porphyrin[19] and benzene[20] was reported in other theoretical studies. Our frontier orbital analysis of conductance is employed to explain observed transport properties in recent experimental studies.[21,22] In the studies of molecular conductance, orbital analysis becomes more and more

† Kyushu University.
‡ The University of Tokyo.

(1) Landauer, R. *IBM J. Res. Dev.* **1957**, *1*, 223.
(2) Datta, S. *Electronic Transport in Mesoscopic Systems*; Cambridge University Press: Cambridge, 1995.
(3) Mujica, V.; Kemp, M.; Roitberg, A.; Ratner, M. *J. Chem. Phys.* **1996**, *104*, 7296.
(4) Samanta, M. P.; Tian, W.; Datta, S.; Henderson, J. I.; Kubiak, C. P. *Phys. Rev. B* **1996**, *53*, R7626.
(5) Magoga, M.; Joachim, C. *Phys. Rev. B* **1997**, *56*, 4722.
(6) Tian, W.; Datta, S.; Hong, S.; Reifenberger, R.; Henderson, J. I.; Kubiak, C. P. *J. Chem. Phys.* **1998**, *109*, 2874.
(7) Olson, M.; Mao, Y.; Windus, T.; Kemp, M.; Ratner, M.; Léon, M.; Mujica, V. *J. Phys. Chem. B* **1998**, *102*, 941.
(8) Cuevas, J. C.; Yeyati, A. L.; Martín-Rodero, A. *Phys. Rev. Lett.* **1998**, *80*, 1066.
(9) Mujica, V.; Roitberg, A. E.; Ratner, M. *J. Chem. Phys.* **2000**, *112*, 6834.
(10) Choi, H. J.; Ihm, J.; Louie, S. G.; Cohen, M. L. *Phys. Rev. Lett.* **2000**, *84*, 2917.
(11) Hall, L. E.; Reimers, J. R.; Hush, N. S.; Silverbrook, K. *J. Chem. Phys.* **2000**, *112*, 1510.
(12) Xue, Y.; Datta, S.; Ratner, M. A. *J. Chem. Phys.* **2001**, *115*, 4292.
(13) Lang, N. D.; Avouris, Ph. *Phys. Rev. B* **2001**, *64*, 125323.
(14) Derosa, P. A.; Seminario, J. M. *J. Phys. Chem. B* **2001**, *105*, 471.
(15) Heurich, J.; Cuevas, J. C.; Wenzel, W.; Schön, G. *Phys. Rev. Lett.* **2002**, *88*, 256803.
(16) Tada, T.; Yoshizawa, K. *ChemPhysChem* **2002**, *3*, 1035.
(17) Tada, T.; Yoshizawa, K. *J. Phys. Chem. B* **2003**, *107*, 8789.
(18) Tada, T.; Nozaki, D.; Kondo, M.; Hamayama, S.; Yoshizawa, K. *J. Am. Chem. Soc.* **2004**, *126*, 14182.
(19) Noda, M.; Watanabe, S. *Jpn. J. Appl. Phys.* **2003**, *42*, L892.
(20) Cardamone, D. M.; Stafford, C. A.; Mazumdar, S. *Nano Lett.* **2006**, *6*, 2422.
(21) Kiguchi, M.; Miura, S.; Hara, K.; Sawamura, M.; Murakoshi, K. *Appl. Phys. Lett.* **2006**, *89*, 213104.
(22) Kiguchi, M.; Miura, S.; Hara, K.; Sawamura, M.; Murakoshi, K. *Appl. Phys. Lett.* **2007**, *91*, 053110.

10.1021/ja800638t CCC: $40.75

effective to understand various electronic features of molecular junctions.[23–45] For example, molecular rectification,[23,24,36,40] molecular switch,[26,28,34,39] conductance modulation by doping,[27,34,41] and field-effect transistor[43] were rationalized by looking at HOMO and LUMO. The purpose of this study is to present the chemical understanding of the electron transport phenomena in molecular junctions on the basis of qualitative orbital thinking. In this paper, we extend the previous discussion[16–18] to an orbital symmetry rule for the transport phenomena using metal−molecule−metal junctions that consist of naphthalene, phenanthrene, and anthracene. Our understanding on the interesting physical phenomena is in line with the orbital concept of frontier orbital theory[46] and the Woodward−Hoffmann rules[47] for chemical reactions.

To look in detail at the applicability of the orbital symmetry rule, we carry out DFT calculations on the molecular junctions of various dithiolate derivatives of naphthalene, phenanthrene, and anthracene. Since the sulfur atom has good affinity with the gold surface, dithiolate derivatives are used for the construction of metal−molecule−metal junctions in general.[21,48–56] The molecule-to-electrodes coupling is relatively strong in these dithiolate molecular junctions because two Au−S bonds mediate the interaction between a molecule and electrodes in these junctions. We investigate whether or not such perturbations can affect the orbital symmetry rule that is derived for weak coupling systems.

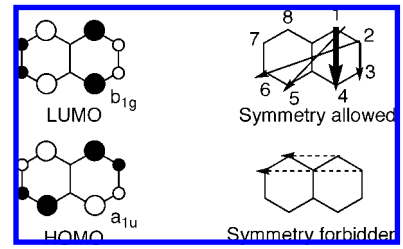

Figure 1. Frontier orbitals of naphthalene and symmetry-allowed and -forbidden routes for electron transmission.

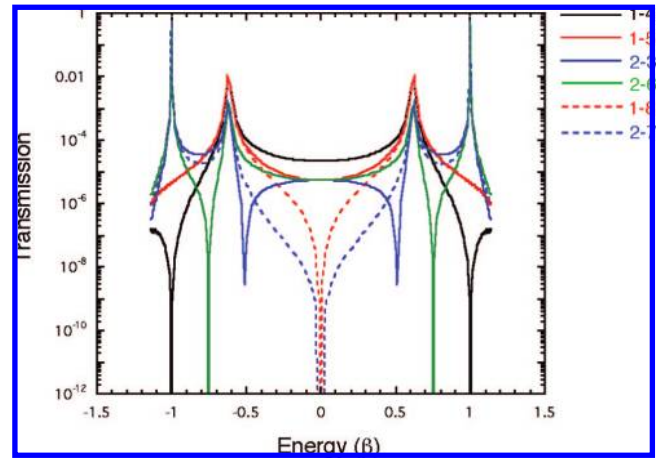

Figure 2. Computed transmission spectra for various routes of a metal−naphthalene−metal junction at the Hückel level of theory.

Role of Frontier Orbitals in Molecular Conductance

Let us consider the electron transport in a metal−molecule−metal junction within the framework of the Hückel method. When two gold chains have contact with atoms r and s of a π-conjugated molecule, the conductance in the zero temperature limit is written as a function of transmission probability between atoms r and s (T_{rs}) at the Fermi energy, as indicated in eq 1.

$$g_{rs} = \frac{2e^2}{h} T_{rs}(E_F) \tag{1}$$

where $2e^2/h$ is the quantum conductance and E_F is the Fermi energy. According to Caroli et al.[57] and Conbescot,[58] the transmission probability can be calculated as follows.

$$T_{rs}(E) = \frac{(2\pi\beta^2_{C-Au})^2}{2} G^A_{sr}(E) G^R_{rs}(E) \rho_\alpha(E) \rho_{\alpha'}(E) \tag{2}$$

where β_{C-Au} is the resonance (transfer) integral between the interacting carbon and gold atoms, G^A and G^R are advanced and retarded Green's functions, respectively, and ρ_α is the local density of states (LDOS) at the interacting gold atom indicated by α. For a weak coupling system, in which there is no chemical

(23) Stokbro, K.; Taylor, J.; Brandbyge, M. *J. Am. Chem. Soc.* **2003**, *125*, 3674.
(24) Larade, B.; Bratkovsky, A. M. *Phys. Rev. B* **2003**, *68*, 235305.
(25) Tagami, K.; Wang, L.; Tsukada, M. *Nano Lett.* **2004**, *4*, 209.
(26) Deng, W.-Q.; Muller, R. P.; Goddard, W. A. *J. Am. Chem. Soc.* **2004**, *126*, 13562.
(27) Senapati, L.; Schrier, J.; Whaley, K. B. *Nano Lett.* **2004**, *4*, 2073.
(28) Kondo, M.; Tada, T.; Yoshizawa, K. *Chem. Phys. Lett.* **2005**, *412*, 55.
(29) Thygesen, K. S.; Jacobsen, K. W. *Phys. Rev. Lett.* **2005**, *94*, 036807.
(30) Ning, Z.; Chen, J.; Hou, S.; Zhang, J.; Liang, Z.; Zhang, J.; Han, R. *Phys. Rev. B* **2005**, *72*, 155403.
(31) Delaney, P.; Nolan, M.; Greer, J. C. *J. Chem. Phys.* **2005**, *122*, 044710.
(32) Choi, Y. C.; Kim, W. Y.; Park, K.-S.; Tarakeshwar, P.; Kim, K. S.; Kim, T. -S.; Lee, J. Y. *J. Chem. Phys.* **2005**, *122*, 094706.
(33) Wu, X.; Li, Q.; Huang, J.; Yang, J. *J. Chem. Phys.* **2005**, *123*, 184712.
(34) Girard, Y.; Kondo, M.; Yoshizawa, K. *Chem. Phys.* **2006**, *327*, 77.
(35) Kondo, H.; Kino, H.; Nara, J.; Ozaki, T.; Ohno, T. *Phys. Rev. B* **2006**, *73*, 235323.
(36) Dalgleish, H.; Kirczenow, G. *Phys. Rev. B* **2006**, *73*, 245431.
(37) Yin, X.; Liu, H.; Zhao, J. *J. Chem. Phys.* **2006**, *125*, 094711.
(38) Kula, M.; Jiang, J.; Lu, W.; Luo, Y. *J. Chem. Phys.* **2006**, *125*, 194703.
(39) Staykov, A.; Nozaki, D.; Yoshizawa, K. *J. Phys. Chem. C* **2007**, *111*, 3517.
(40) Staykov, A.; Nozaki, D.; Yoshizawa, K. *J. Phys. Chem. C* **2007**, *111*, 11699.
(41) Ono, T.; Hirose, K. *Phys. Rev. Lett.* **2007**, *98*, 026804.
(42) Chen, L.; Hu, Z.; Zhao, A.; Wang, B.; Luo, Y.; Yang, J.; Hou, J. G. *Phys. Rev. Lett.* **2007**, *99*, 146803.
(43) Perrine, T. M.; Dunietz, B. D. *Phys. Rev. B* **2007**, *75*, 195319.
(44) Ning, J.; Qian, Z.; Li, R.; Hou, S.; Rocha, A. R.; Sanvito, S. *J. Chem. Phys.* **2007**, *126*, 174706.
(45) Calzolari, A.; Ferretti, A.; Nardelli, M. B. *Nanotechnology* **2007**, *18*, 424013.
(46) Fukui, K. *Theory of Orientation and Stereoselection*; Springer: Berlin, 1970.
(47) Woodward, R. B.; Hoffmann, R. *The Conservation of Orbital Symmetry*; Verlag Chemie GmbH: Weinheim, Germany, 1970.
(48) Reed, M. A.; Zhou, C.; Muller, C. J.; Burgin, T. P.; Tour, J. M. *Science* **1997**, *278*, 252.
(49) Cui, X. D.; Primak, A.; Zarate, X.; Tomfohr, J.; Sankey, O. F.; Moore, A. L.; Moore, T. A.; Gust, D.; Harris, G.; Lindsay, S. M. *Science* **2001**, *294*, 571.
(50) Reichert, J.; Ochs, R.; Beckmann, D.; Weber, H. B.; Mayer, M.; Löhneysen, H. v. *Phys. Rev. Lett.* **2002**, *88*, 176804.
(51) Kushmerick, J. G.; Holt, D. B.; Yang, J. C.; Naciri, J.; Moore, M. H.; Shashidhar, R. *Phys. Rev. Lett.* **2002**, *89*, 086802.
(52) Zhitenev, N. B.; Meng, H.; Bao, Z. *Phys. Rev. Lett.* **2002**, *88*, 226801.
(53) Xiao, X.; Xu, B.; Tao, N. J. *Nano Lett.* **2004**, *4*, 267.
(54) Dadosh, T.; Gordin, Y.; Krahne, R.; Khivrich, I.; Mahalu, D.; Frydman, V.; Sperling, J.; Yacoby, A.; Bar-Joseph, I. *Nature* **2005**, *436*, 677.
(55) Fujihira, M.; Suzuki, M.; Fujii, S.; Nishikawa, A. *Phys. Chem. Chem. Phys.* **2006**, *8*, 3876.
(56) Lörtscher, E.; Weber, H. B.; Riel, H. *Phys. Rev. Lett.* **2007**, *98*, 176807.
(57) Caroli, C.; Combescot, R.; Nozieres, P.; Saint-James, D. *J. Phys. C* **1971**, *4*, 916.
(58) Combescot, R. *J. Phys. C* **1971**, *4*, 2611.

bonding between the molecule and electrodes, Green's function can be obtained from zeroth Green's functions separately calculated for the electrodes and molecule. As the electrodes we used a linear gold chain, and Green's function at the α site can be obtained analytically as follows.

$$g_L^{R/A}(E) = g_R^{R/A}(E) = \frac{\pm i}{2\beta_{\mathrm{Au-Au}}} \frac{(1 - \exp[\pm i 2y_0])}{\sin y_0} \tag{3}$$

where $\beta_{\mathrm{Au-Au}}$ is the resonance integral between nearest neighboring gold atoms and y_0 satisfies the condition of $E/2\beta_{\mathrm{Au-Au}} - \cos y_0 = 0$.[59] The matrix elements of zeroth Green's function for the molecular part have the following form.

$$G^{(0)R/A}_{rs}(E) \sum_k \frac{C_{rk} C^*_{sk}}{E - \epsilon_k \pm i\eta} \tag{4}$$

where C_{rk} is the kth MO expansion coefficient at site r, and ϵ_k is the kth MO energy. Green's functions in eq 2 are considered to be a linear function of zeroth Green's function of eq 4 in weak coupling systems. Details of this procedure are described in a previous paper.[17] If we assume the Fermi energy to be located at the midgap of the HOMO and LUMO, we can qualitatively characterize the transmission probability by looking at the HOMO and LUMO because the contributions of the HOMO and LUMO indicated in eq 5 are significant in zeroth Green's function for the molecule at the Fermi energy. Although the definition of the Fermi energy will affect general profiles of the transmission spectra, we think that this simple definition is a good starting point for qualitative discussion based on this simple model.

$$\frac{C_{r\mathrm{HOMO}} C^*_{s\mathrm{HOMO}}}{E_{\mathrm{F}} - \varepsilon_{\mathrm{HOMO}} \pm i\eta} + \frac{C_{r\mathrm{LUMO}} C^*_{s\mathrm{LUMO}}}{E_{\mathrm{F}} - \varepsilon_{\mathrm{LUMO}} \pm i\eta} \tag{5}$$

Let us first consider the electron transport properties in naphthalene. The HOMO and LUMO of naphthalene are shown in Figure 1. Note that there is electron−hole symmetry or pairing theorem[60] with respect to MO energies and MO expansion coefficients of alternant hydrocarbons within the framework of the Hückel method, in which the overlap integral is neglected. We can predict from their orbital phase and amplitude that the two terms of eq 5 are enhanced in certain connections of atoms and canceled in other connections. Since the signs of the denominators $E_{\mathrm{F}} - \epsilon_{\mathrm{HOMO}}$ and $E_{\mathrm{F}} - \epsilon_{\mathrm{LUMO}}$ are different, when the sign of product $C_{r\,\mathrm{HOMO}} C^*_{s\,\mathrm{HOMO}}$ is different from that of product $C_{r\,\mathrm{LUMO}} C^*_{s\,\mathrm{LUMO}}$, the contributions from the HOMO and LUMO are enhanced. On the other hand, when the sign of product $C_{r\,\mathrm{HOMO}} C^*_{s\,\mathrm{HOMO}}$ is the same as that of product $C_{r\,\mathrm{LUMO}} C^*_{s\,\mathrm{LUMO}}$, the contributions from the HOMO and LUMO are canceled. This relationship holds true also in a pair of HOMO−1 and LUMO+1, a pair of HOMO−2 and LUMO+2, and so on, due to the electron−hole symmetry at this level of theory. In order to further enhance the contributions from the HOMO and LUMO, two atoms in which the amplitude of the HOMO and LUMO is large should be connected with electrodes.

Thus, the transmission probability depends on how two gold chains are connected with the molecule. On the basis of the qualitative thinking about the orbital phase, we can easily predict symmetry-allowed and symmetry-forbidden connections for transmission probability in naphthalene, as shown in Figure 1. The solid arrows show connections in which we expect finite transmission probability, and the dotted arrows show connections in which we expect no transmission probability. Note that orbital phase is essential for the characterization of this simple rule. As shown by the thick arrow, connection 1-4 (also 5-8) is predicted to be the best route for electron transport in naphthalene because the sign of product $C_{1\,\mathrm{HOMO}} C^*_{4\mathrm{HOMO}}$ is different from that of product $C_{1\,\mathrm{LUMO}} C^*_{4\mathrm{LUMO}}$ and the HOMO and LUMO are localized at sites 1 and 4 (also at sites 5 and 8).

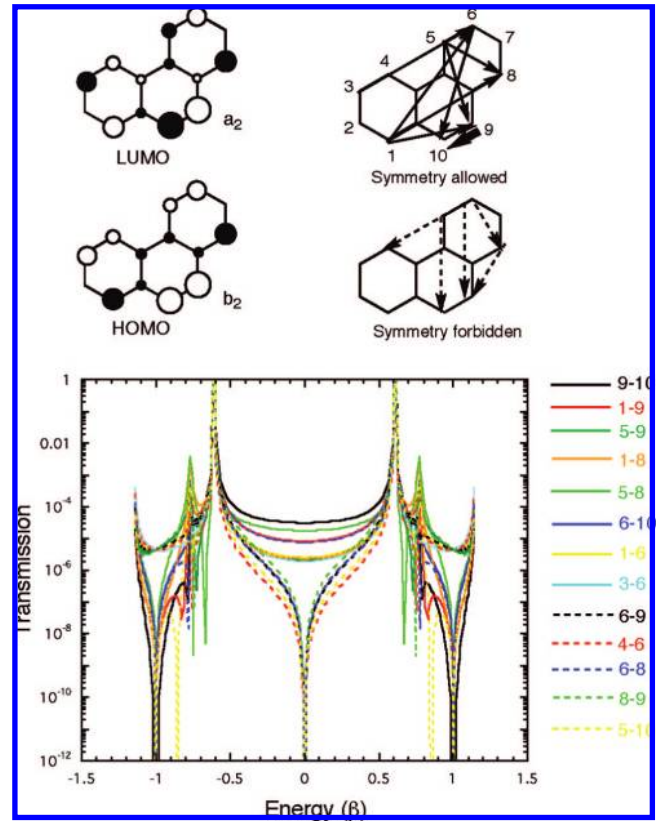

Figure 3. Frontier orbitals of phenanthrene and symmetry-allowed and -forbidden routes for electron transmission. Computed transmission spectra for various routes of a metal−phenanthrene−metal junction at the Hückel level of theory.

Having described the qualitative orbital symmetry rule for the electron transport in naphthalene, let us next look at computational results at the Hückel level of theory. Computed transmission spectra for various connections of naphthalene are shown as a function of the energy of electron in Figure 2, where the solid lines show symmetry-allowed connections and the dotted lines show symmetry-forbidden connections. The sharp transmission peaks come from the resonance tunneling effect at the location of MO levels. The transmission probability at the Fermi energy ($E = 0$) plays an important role in conductance, as mentioned earlier in eq 1. This computational result is fully consistent with the qualitative prediction based on the orbital symmetry discussion. As we expect, connection 1-4 has the largest transmission probability at the Fermi energy, whereas connections 1-8 and 2-7 have no transmission probability. Connections 1-5, 2-3, and 2-6 have similar transmission probabilities at the Fermi energy. The transmission probability in the symmetry-forbidden connections 1-8 and 2-7 is computed to be zero because zeroth Green's function of eq 4 is canceled owing to the electron−hole symmetry within the framework of the Hückel method.

(59) Emberly, E. G.; Kirczenow, G. *J. Phys.: Condens. Matter* **1999**, *11*, 6911.
(60) Dewar, M. J. S. *The Molecular Orbital Theory of Organic Chemistry*; McGraw-Hill: New York, 1969.

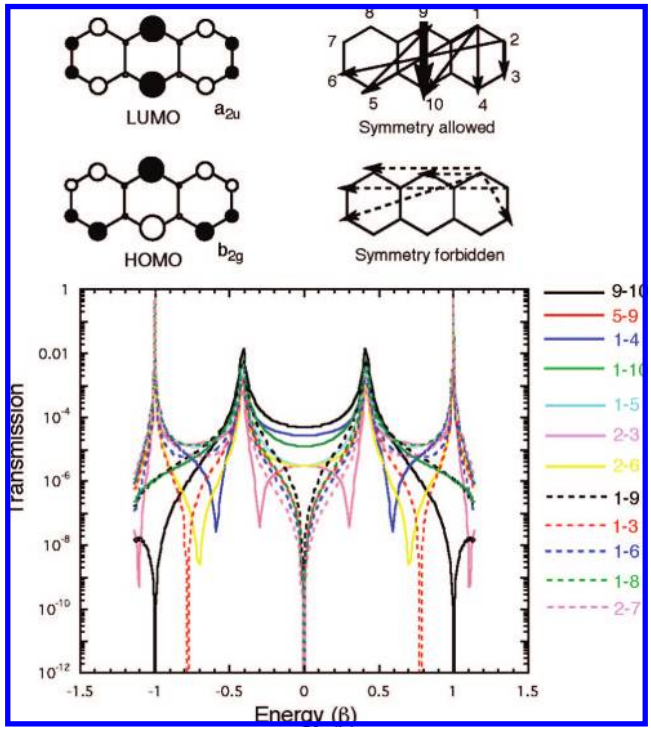

Figure 4. Frontier orbitals of anthracene and symmetry-allowed and -forbidden routes for electron transmission. Computed transmission spectra for various routes of a metal−anthracene−metal junction at the Hückel level of theory.

In the same way, we are able to distinguish between symmetry-allowed and symmetry-forbidden connections for the transmission probability in phenanthrene and anthracene. Our qualitative predictions are in excellent agreement with transmission spectra computed at the Hückel level of theory, as shown in Figures 3 and 4. In phenanthrene, connection 9-10 has the largest transmission probability and connection 5-8 has the second largest one, whereas connections 6-9, 4-6, 6-8, 8-9, and 5-10 have no transmission probability because zeroth Green's function is canceled. In anthracene, connection 9-10 has the largest transmission probability and connection 1-4 has the second largest one, but electron transmission is forbidden in connections 1-9, 1-3, 1-6, 1-8, and 2-7.

Thus, the orbital symmetry rule is very useful for the prediction of essential electron transport phenomena in π-conjugated molecules. This rule can be summarized as follows: (1) the sign of product $C_{r\,\mathrm{HOMO}}C^{*}_{s\,\mathrm{HOMO}}$ should be different from the sign of product $C_{r\,\mathrm{LUMO}}C^{*}_{s\,\mathrm{LUMO}}$, where r and s are atom indices, and (2) atoms r and s in which the amplitude of the HOMO and LUMO is large should be connected. We can mention condition (1) in another way in terms of alternant hydrocarbon; *starred* and *unstarred* atoms should be connected. Here a π-conjugate system is termed alternant if the atoms in it can be divided into two groups, *starred* and *unstarred*, in such a way that no two atoms of the same group are directly linked.[60] The chemical understanding of electron transport properties in molecular junctions in terms of the orbital concept is of great value, we think.

DFT Calculations of Molecular Conductance

The necessary conditions to derive the orbital symmetry rule discussed in the previous section are that (1) the coupling between the molecule and electrodes is weak, (2) there is electron−hole symmetry in orbital energies and orbital expansion coefficients, and (3) the Fermi energy is located at the midgap of the HOMO and LUMO. When these assumptions do not hold true, the qualitative discussion might fail. We therefore performed more quantitative calculations using realistic molecular junctions with the nonequilibrium Green's function (NEGF)−DFT method implemented in the ATK 2.3 program[61–63] in order to look at the qualitative predictions based on the phase and amplitude of the HOMO and LUMO. The method includes full self-consistent-field (SCF) treatment of metal−molecule−metal junctions, in which two gold electrodes are strongly interacted with possible dithiolate derivatives of naphthalene, phenanthrene, and anthracene through Au−S chemical bonds. This situation is a little different from assumption (1). The adsorption site of the dithiolate derivatives adopted in this study is the fcc three-fold hollow site. The semi-infinite left and right electrodes were modeled by two Au(111)-(3 × 3) surfaces (i.e., each layer includes nine Au atoms). The two probe models we used for the scattering region include 99 atoms from the Au(111) electrodes; 5 layers and 6 layers were used for the left- and right-hand sides, respectively. To save computational efforts, a single-ζ basis function was used for the gold atoms and double-ζ basis functions with polarization were used for all other atoms of the molecular part.[61] The exchange-correlation potential described by the Perdew−Zunger local density approximation was used.[64] Single k-point sampling on the plain perpendicular to the direction of the current was used for both NEGF-SCF iterations and transmission calculations. We confirmed that computations with more k-points do not affect the conclusions. The $I-V$ curves reported in the present study were obtained after sequences of SCF calculations for applied biases in the range from 0.0 to 1.0 V. The geometries of all investigated structures were in advance fully optimized at the B3LYP-DFT level of theory[65–68] implemented in the Gaussian 03 program.[69] Models for geometry optimization include one Au atom from the electrodes connected to each S atom. The 6-31G* basis set[70] was used for the C, H, and S atoms, and the LANL2DZ basis set[71] was used for the Au atoms.

Electron Transport in Naphthalene Dithiolates. Four kinds of dithiolate derivatives are possible for naphthalene as molecular wires while 1,8- and 2,3-naphthalene dithiolates are not appropriate because the distance between the two sulfur atoms is too close in these derivatives. We demonstrate in Figure 5 zero-bias transmission spectra for the possible dithiolate derivatives of naphthalene computed at the Perdew−Zunger LDA level of theory. The Fermi energy ($E = 0$) in this figure was determined from DFT calculations of the bulk gold electrodes. The Fermi energy thus calculated intersects the transmission peaks that originate from the resonance tunneling with the HOMOs of the dithiolates. Although the Fermi energy is located

(61) Brandbyge, M.; Mozos, J.-L.; Ordejon, P.; Taylor, J.; Stokbro, K. *Phys. Rev. B* **2002**, *65*, 165401.
(62) *ATK*, version 2.3, atomistix a/s; www.atomistix.com.
(63) Taylor, J.; Guo, H.; Wang, J. *Phys. Rev. B* **2001**, *63*, 245407.
(64) Perdew, J.; Zunger, A. *Phys. Rev. B* **1981**, *23*, 5048.
(65) Frisch, M. J. *Gaussian 03*, revision B.03; Gaussian, Inc.: Wallingford CT, 2004.
(66) Becke, A. *J. Chem. Phys.* **1993**, *98*, 5648.
(67) Lee, C.; Yang, W.; Parr, R. *Phys. Rev. B* **1988**, *37*, 785.
(68) Vosko, S.; Wilk, L.; Nusair, M. *Can. J. Phys.* **1980**, *58*, 1200.
(69) Stephens, P.; Devlin, F.; Chabalowski, C.; Frisch, M. J. *J. Phys. Chem.* **1994**, *98*, 11623.
(70) Krishnan, R.; Binkley, J.; Seeger, R.; Pople, J. A. *J. Chem. Phys.* **1980**, *72*, 650.
(71) Hay, P.; Wadt, W. *J. Chem. Phys.* **1985**, *82*, 270.

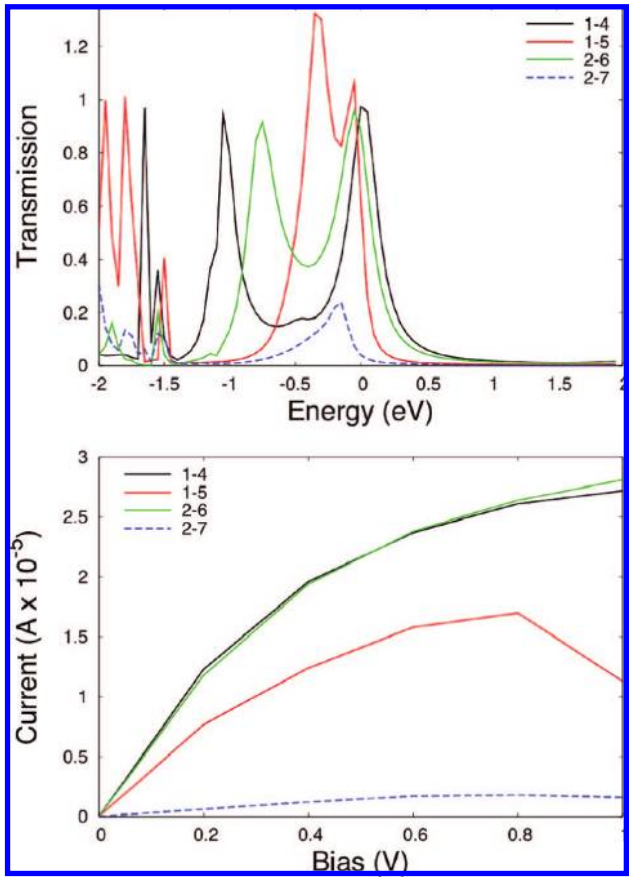

Figure 5. Computed transmission spectra and $I-V$ curves for naphthalene dithiolate junctions at the Perdew−Zunger LDA level of theory.

in the gap of the HOMO and LUMO, it is nearer to the HOMO. As we expect, 1,4-naphthalene dithiolate has a transmission probability of nearly 1 at the Fermi energy; therefore, it is the best derivative from the viewpoint of conductance. Computed transmission probabilities for symmetry-allowed connections 1,5- and 2,6-naphthalene dithiolates are about 0.5 and 0.8, respectively, whereas that for symmetry-forbidden connection 2,7-naphthalene dithiolate is nearly 0. These results are in excellent agreement with the qualitative prediction made from the phase and amplitude of the HOMO and LUMO of naphthalene. Computed $I-V$ curves are also consistent with the orbital symmetry rule, as demonstrated in Figure 5.

In 1,5-naphthalene dithiolate, the transmission coefficient for the second peek under the Fermi energy exceeds unity. In such a case, there are multiple transmission channels for the same energy in general. These are the HOMO and HOMO−1 just under the Fermi energy. We performed a molecular projected self-consistent Hamiltonian (MPSH) analysis, which shows us the spatial distribution of orbital levels modified by the electrodes. The HOMO level is well delocalized for all structures giving the peak under the Fermi energy except 2,7-naphthalene dithiolate. The HOMO−1 is delocalized only in 1,5-naphthalene dithiolate, giving the second peak under the Fermi energy. For all other structures, the HOMO−1 is well localized and gives no peak of transmission. Because the HOMO and HOMO−1 in 1,5-naphthalene dithiolate are very close in energy, they both contribute to the transmission for one and the same energy. Computed MPSH levels corresponding to the HOMO and HOMO−1 of 1,4- and 1,5-naphthalene dithiolates are compared in Figure 6, where orbitals extended to the electrodes are cut

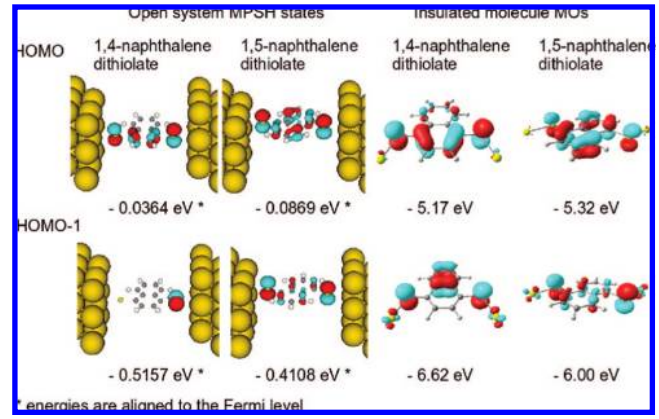

Figure 6. MPSH levels corresponding to the HOMO and HOMO−1 of 1,4- and 1,5-naphthalene dithiolates for zero bias and the corresponding orbitals of the insulated molecules.

for clarity. The HOMOs of 1,4- and 1,5-naphthalene dithiolates clearly derive from the HOMO of naphthalene (see Figure 1), indicating that the frontier orbital properties for electron transport are conserved between naphthalene and its dithiolate derivatives. Therefore, the qualitative prediction of electron transport evaluated in the weak molecule−metal contact works well even in the contact mediated by Au−S bonds. The HOMO and HOMO−1 levels of the insulated molecules with one gold atom bonded to each terminal sulfur atom are also shown in Figure 6. In the case of 1,5-naphthalene dithiolate, the spatial distribution of both the HOMO and HOMO−1 levels is very close to the calculated MPSH levels. This is also true for the HOMO of 1,4-naphthalene dithiolate. Its HOMO−1 lies lower in the energy spectrum of the insulated molecule, and in the open system, the HOMO−1 level is a state localized on one of the electrodes and the anchoring S atom.

Although the orbital symmetry rule is a powerful tool in the qualitative prediction of electron transport, it is hard from the orbital symmetry rule to predict $I-V$ properties that sometimes show unexpected responses especially in highly biased systems. In the $I-V$ curve of 1,5-naphthalene dithiolate, a drop in the calculated current with an increase in applied bias is observed from 0.8 to 1.0 V. This is a negative differential resistance (NDR) effect in a molecular junction. In usual $I-V$ curves, current increases with an increase in applied bias because, in general, the transmission spectrum for applied bias remains almost unchanged from that for zero bias. Thus, when a larger bias is applied, the expanded bias window (BW) contributes to a larger value of current because the current satisfies the following equation at 0 K.

$$I(V) = \frac{2e}{h}\int_{\mathrm{BW}} \mathrm{d}ET(E, V) \qquad (6)$$

However, the condition that the transmission spectrum does not significantly change with applied bias is not always true. Effects of the external electric field, which are included in the present NEGF-DFT calculations,[62] can localize "conductance" levels near one of the electrodes. Localized "non-conductance" levels will lead to a smaller integration area under the peak in the transmission spectrum that cannot be compensated by the increased bias window. As a result, a lower value of current can be calculated. This is the case with 1,5-naphthalene dithiolate, where the HOMO is delocalized for biases up to 0.8 V while localized for 1.0 V bias. The transmission spectra for 1,5-naphthalene dithiolate for applied biases of 0.8 and 1.0 V

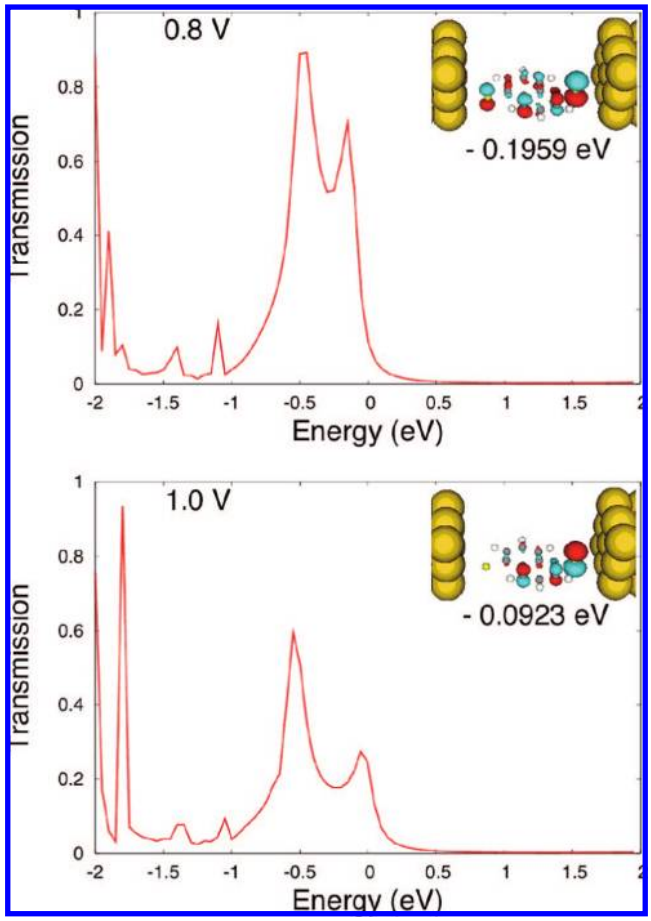

Figure 7. Computed transmission spectra and MPSH levels corresponding to the HOMO of 1,5-naphthalene dithiolate for applied biases of 0.8 and 1.0 V, respectively.

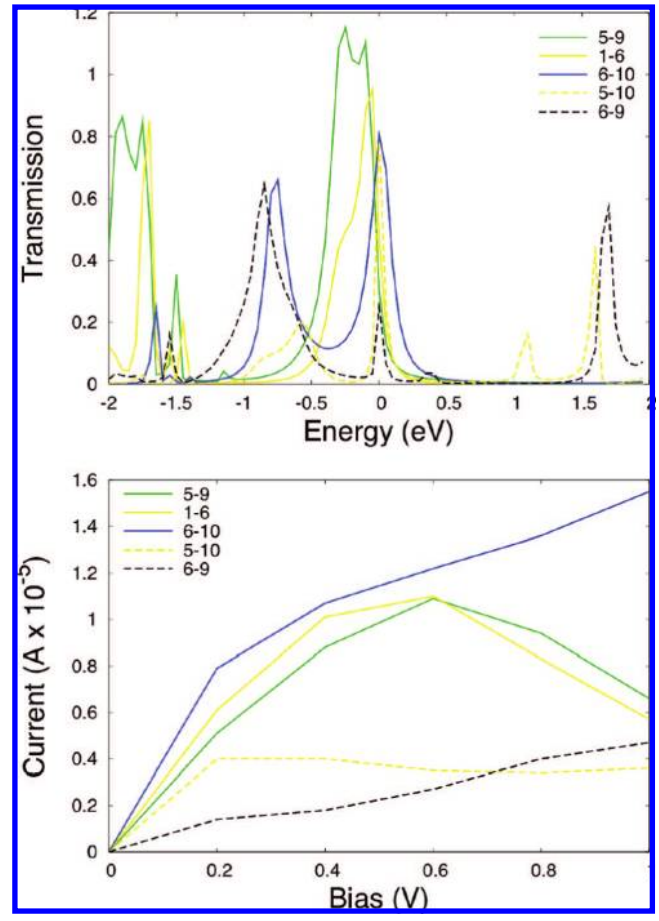

Figure 8. Computed transmission spectra and $I-V$ curves for phenanthrene dithiolate junctions at the Perdew−Zunger LDA level of theory.

are compared in Figure 7, in which computed MPSH levels corresponding to the HOMOs are visualized.

Electron Transport in Phenanthrene Dithiolates. Here we considered five kinds of dithiolate derivatives of phenanthrene that are possible as molecular wires. The 9-10 connection that we expect the highest transmission probability is not appropriate for the formation of dithiolate because the distance between the two sulfur atoms is too close in 9,10-phenanthrene dithiolate. The 5-8 connection is also not appropriate as a molecular wire because the H atom at the 3 position interferes with an electrode. So we calculated 5,9-, 1,6-, and 6,10-phenanthrene dithiolates that we expect symmetry-allowed connections for electron transport and 5,10- and 6,9-phenanthrene dithiolates that we predict symmetry-forbidden connections. Figure 8 shows computed zero bias transmission spectra and $I-V$ curves for these phenanthrene dithiolates. Computed $I-V$ curves clearly demonstrate that the qualitative predictions are in good agreement with the present DFT results. In 5,9-phenanthrene dithiolate, the transmission coefficients for the first and second peek under the Fermi energy exceed unity such as in 1,5-naphthalene dithiolate. Also, in this case, the HOMO and HOMO−1 are very close in energy, and they both contribute to the transmission for one and the same energy. The drops of the calculated current in the $I-V$ curves of 5,9- and 1,6-phenanthrene dithiolates are a result of the localization of conductance levels for higher biases such as in 1,5-naphthalene dithiolate.

Electron Transport in Anthracene Dithiolates. Five kinds of dithiolate derivatives of anthracene possible as molecular wires were considered here: 1,5-, 1,10-, 2,6-, and 9,10-anthracene dithiolates that we expect high transmission probability and 2,7-anthracene dithiolate that we expect poor transmission probability. Computed transmission probabilities and $I-V$ curves for the dithiolate derivatives of anthracene are shown in Figure 9. In view of the transmission spectra and the $I-V$ curves, 1,5- and 2,6-anthracene dithiolates show high conductance and 2,7-anthracene dithiolate shows poor conductance, as expected. However, the computed results for 9,10- and 1,10-anthracene dithiolates are not in agreement with our qualitative predictions, in particular, in connection 9-10. Although the orbital symmetry rule tells us that connection 9-10 should give the highest transmission probability, the dithiolate derivative corresponding to connection 9-10 does not show excellent transmission probability. The reason for this disagreement is quite clear. First of all, optimized C−S bond distances of 1.66 Å in the corresponding 9,10-anthracene dithiolate are very short in comparison with those of 1.80−1.85 Å in the other dithiolates. The short C−S bonds of 9,10-anthracene dithiolate should be viewed as a double bond, therefore this structure being better described as a dithioquinone. Since such a system is significantly perturbed, and the original π-conjugation network should be extended in the prediction of electron transport. In order to confirm this, we extended the π-conjugation network of anthracene and calculated the transmission spectra at the Hückel level of theory by adding two extra carbon atoms. Computed transmission functions between the two added atoms at the 2,6, 1,5, and 9,10 sites are 7.8×10^{-4}, 7.8×10^{-4}, and 4.9×10^{-5} at the Fermi energy, respectively. This result is in good

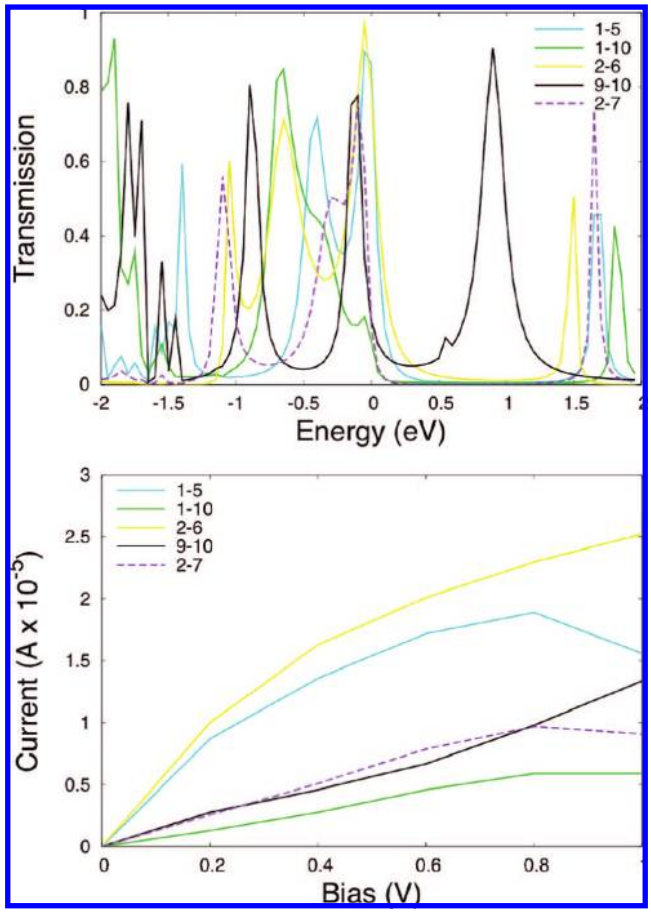

Figure 9. Computed transmission spectra and $I-V$ curves for anthracene dithiolate junctions at the Perdew−Zunger LDA level of theory.

agreement with the NEGF-DFT result shown in Figure 9. Since an eventual extension of π-conjugation network can lead to different frontier orbitals, we must take care about the spatial extent of π-conjugation network in the prediction for strong coupling systems.

Although anthracene belongs to the stable $(4n + 2)\pi$ system, it shows high reactivity, due to the small energy difference of the HOMO and LUMO and their strong localization at the central two carbon atoms at the 9 and 10 positions.[72] For example, anthracene is converted to anthraquinone by CrO_3; it reacts with dienophiles to form [4 + 2] cycloadducts, and it is transformed to a dimer upon photoirradiation. These reactions show the high reactivity of anthracene at the 9 and 10 positions. Thus, anthracene and larger acenes can be viewed as an exceptional series in aromatic compounds. Interestingly, the frontier electron density analysis by Fukui et al.[73] is not successful for the correct prediction of observed products in the sulfonation of anthracene.

Summary and Conclusions

We propose an orbital symmetry rule for electron transport properties in π-conjugated molecules, demonstrating that the phase and amplitude of the HOMO and LUMO play an essential role in the physical phenomena. Qualitative predictions based on the orbital concept, which physicists have been unlikely to use, are of great value in a better understanding of the electron transport phenomena in single-molecular devices. For large transmission probability, (1) *starred* and *unstarred* atoms should be connected in terms of alternant hydrocarbon, and (2) atoms in which the amplitude of the HOMO and LUMO is large should be connected. This rule allows us to predict essential transport properties in molecular junctions. We compared qualitative predictions based on frontier orbital analysis about the site-dependent electron transport in naphthalene, phenanthrene, and anthracene with DFT calculations for the molecular junctions of their dithiolate derivatives, in which gold electrodes have relatively strong contact with a molecule through two Au−S bonds. Our predictions made for weak coupling systems are almost all consistent with the DFT results, except for some anthracene dithiolate derivatives that involve sulfur atoms at the central 9 or 10 position. In these exceptions, the C−S bonds are extremely short by approximately 0.2 Å compared with those of other dithiolate derivatives, and as a result, the original π-conjugation network is extended and perturbed. Thus, the orbital concept works well in the prediction of electron transport when the nature of frontier orbitals is not significantly affected by strong coupling between a molecule and electrodes. Since essential orbital natures are very similar among Hückel, extended Hückel, Hartree−Fock, and DFT calculations especially about symmetry,[74] the qualitative orbital views are useful in rationalizing the electron transport phenomena in molecular junctions. Finally, we would like to refer to recent experimental findings that tell us the predictive power of the orbital symmetry rule in designing molecular devices. The conductances of 1,4-benzenedithiol (S−C_6H_4−S), 1,4-diisocyanobenzene (CN−C_6H_4−NC), and 1,4-dicyanobenzene (NC−C_6H_4−CN) sandwiched between gold electrodes were measured using scanning tunneling microscope (STM), and the highest conductance was found in the benzenedithiol junction.[21] The conductance variation depending on the anchor group (−S, −NC, and −NC) is successfully analyzed by the frontier orbital views. Enhancement of conductance was reported when a single molecule was attached to platinum electrodes instead of gold electrodes. The frontier orbital concept for electron transport is again employed to understand the enhancement of conductance.[22] We would like to know whether our predictions are correct or not experimentally in further examples.

Note: Qualitative orbital analyses based on Hückel calculations show a high conductance for the 1-4 connection in comparison with those for the 1-5 and 2-6 connections in naphthalene, while in NEGF-DFT calculations 1-4 and 2-6 naphthalene dithiolates show nearly identical conductances, which are higher than that for 1-5 naphthalene dithiolte. DFT calculations of these dithiolates, in which each sulfur atom is terminated with a gold atom, show that the HOMOs are well delocalized on the whole molecules, whereas the LUMOs are localized on the contact regions of Au−S. In general, such delocalized orbitals play an important role in electron transport. Moreover, the energies of the HOMOs are closer to the Fermi energy of the gold electrodes; thus, the HOMOs would offer main transmission channels through the molecules. Therefore, the Au–S bonds in the dithiolates will work as "orbital filtering" for electron transport.

We have to look at the HOMOs of the naphthalene dithiolates rather than the combinations of the HOMOs and LUMOs in considering electron transport properties because the HOMOs

(72) Yoshizawa, K.; Yahara, K.; Tanaka, K.; Yamabe, T. *J. Phys. Chem. B* **1998**, *102*, 498.
(73) Fukui, K.; Yonezawa, T.; Shingu, H. *J. Chem. Phys.* **1952**, *20*, 722.
(74) Stowasser, R.; Hoffmann, R. *J. Am. Chem. Soc.* **1999**, *121*, 3414.

are well delocalized and closer to the Fermi energy of the electrodes, as mentioned above. The HOMOs of the naphthalene dithiolates have finite amplitude on the sulfur atoms, as shown in Figure S1 in the Supporting Information. These dithiolates are therefore considered to have similar electron transport properties. Slight differences in the transport properties found in the NEGF-DFT calculations would come from the type of coupling between the sulfur and gold atoms. In Figure S1, the HOMOs of 1-4 and 2-6 naphthalene dithiolates have small amplitude on the gold atoms, whereas the HOMO of 1-5 naphthalene dithiolate has no amplitude on the gold atoms. Thus, 1-4 and 2-6 naphthalene dithiolates have higher transmission probabilities than 1-5 naphthalene dithiolate.

The discussion made above is about a comparison among the symmetry-allowed connections for naphthalene. On the other hand, a large difference of conductance between the symmetry-allowed 1-4 and symmetry-forbidden 2-7 connections is clearly seen in NEGF-DFT calculations for the corresponding naphthalene dithiolates. Thus, the frontier orbitals of naphthalene are of great use in understanding the essential electron transport properties of the dithiolate derivatives. This is also true for the phenanthrene dithiolates. The breakdown of the symmetry rule in the anthracene dithiolates comes from a different reason, as discussed above.

Acknowledgment. This work was supported by Grants-in-Aid for Scientific Research (Nos. 18350088, 18066013, and 18GS0207) from the Japan Society for the Promotion of Science, the Global COE Project, the Nanotechnology Support Project, the Joint Project of Chemical Synthesis Core Research Institutions from the Ministry of Culture, Sports, Science, and Technology of Japan (MEXT), and CREST of the Japan Science and Technology Cooperation.

Supporting Information Available: Parameters for Hückel calculations: $\beta_{Au-Au} = 0.6\beta_{C-C}$ and $\beta_{C-Au} = 0.2\beta_{C-C}$. Complete ref 65, calculated HOMOs of Au_2(naphthalene dithiolates), and atomic Cartesian coordinates and absolute energies (in Hartree) for all the structures optimized in the present study. This material is available free of charge via the Internet at http://pubs.acs.org.

JA800638T